

General Pathways to Higher Order Compensation Circuits for IPT Converters via Sensitivity Analysis

Ying Cathy Liu [✉], *Student Member, IEEE*, Jiantao Zhang, Chi K. Tse [✉], *Fellow, IEEE*, Chunbo Zhu, and Siu-Chung Wong [✉], *Senior Member, IEEE*

Abstract—This article first presents a systematic extension of second-order compensated inductive power transfer (IPT) converters, designed for achieving load-independent current (LIC) or load-independent voltage (LIV) output, to third-order compensated IPT converters through adding an inductor or capacitor at the input or output side. Conditions on the parameters to achieve the required output are given. Then, the system sensitivity to various parameter fluctuation is analyzed. Results from sensitivity analysis provide a convenient design guide for selecting parameters to achieve the required LIV and LIC operation for higher order IPT systems with fewer design constraints. Moreover, the analysis effectively reveals the roles of extra input-side or output-side inductors and capacitors in making the whole system less sensitive, and hence provides a fast understanding of the choice of higher order compensation circuits for applications addressing wide ranges of input variations, transformer coupling, and compensation network changes.

Index Terms—Compensation, inductive power transfer (IPT) converters, load-independent current (LIC)/voltage output, sensitivity analysis.

I. INTRODUCTION

INDUCTIVE power transfer (IPT) has been used in a variety of applications such as battery charging in electric vehicles, power supplies for consumer electronics, transcutaneous power supplies, and so on [1]–[5]. In many practical applications, the power supply terminals are required to provide either constant voltage (CV) or constant current (CC), and in some applications, such as battery charging, the power supply is required to provide both CV and CC depending on the operating phase of the

Manuscript received September 28, 2020; revised November 26, 2020 and January 18, 2021; accepted February 22, 2021. Date of publication February 25, 2021; date of current version June 1, 2021. This work was supported in part by Hong Kong RGC theme-based research under Grant T23-701-20-R and in part by a Joint Ph.D. Program of Hong Kong Polytechnic University and Harbin Institute of Technology. Recommended for publication by Associate Editor M. Vitelli. (*Corresponding author: Jiantao Zhang.*)

Ying Cathy Liu is with the Department of Electrical Engineering and Automation, Harbin Institute of Technology, Harbin, China, and also with the Department of Electronic and Information Engineering, Hong Kong Polytechnic University, Hong Kong (e-mail: cathy-ying.liu@connect.polyu.hk).

Jiantao Zhang and Chunbo Zhu are with the Department of Electrical Engineering and Automation, Harbin Institute of Technology, Harbin 150001, China (e-mail: jiantaoz@hit.edu.cn; zhuchunbo@hit.edu.cn).

Chi K. Tse is with the Department of Electrical Engineering, City University of Hong Kong, Hong Kong (e-mail: ckse@ieee.org).

Siu-Chung Wong is with the Department of Electronic and Information Engineering, Hong Kong Polytechnic University, Hong Kong (e-mail: escwong@polyu.edu.hk).

Color versions of one or more figures in this article are available at <https://doi.org/10.1109/TPEL.2021.3062228>

Digital Object Identifier 10.1109/TPEL.2021.3062228

charging process [6], [7], as the equivalent resistance of the battery varies significantly during the charging process. In order to operate in a wide load range, various compensation topologies are applied in IPT systems to achieve load-independent current (LIC) and load-independent voltage (LIV) output. Research on basic second-order compensation has already entered a mature stage. It is well known that four basic compensation topologies, namely, series/series (S/S), series/parallel (S/P), parallel/series (P/S), and parallel/parallel (P/P) configurations, can achieve LIC or LIV output at specific operating frequencies [8], [9]. Further study of the basic compensation networks for both LIC and LIV output has been conducted [10], and a series of optimization design based on the second-order compensations have been proposed [11]–[13]. Moreover, to enhance the operating range and to combat parameter variations, higher order compensations are used. For example, Fig. 1(a) shows four types of third-order compensated IPT converters. In [14], a family of higher order compensation topologies have been studied. While achieving LIC or LIV output, these topologies, interpreted in terms of transformer model (T-model) or mutual inductance model (M-model), show good performance in combating the transformer parameter constraints. Specifically, an *LCL* compensated IPT system has been proposed to provide constant primary current, which is particularly suitable for multipickup applications [15]–[17]. Furthermore, an *LCC* compensation network has been utilized to enhance the tolerance for lateral misalignment and permits reduction of system size [18]. However, despite the many individual reports focusing on the use of higher order compensation in combating parameter variation [14], [19], [20], there is still a lack of systematic analysis with clear physical meanings that can guide engineers to design compensation circuits more effectively. In the work of Lu *et al.* [21], sensitivity analysis of voltage gain and efficiency to variation in system parameters has been carried out for various topologies operating in CV mode, aiming at simplifying the control algorithm and minimizing additional converters. The essential connection between second-order and higher order compensation circuits remains unattended. Recently, the transformation between second-order and third-order compensation circuits at the input side, based on sensitivity analysis of selected topologies, has been briefly discussed [22]. Up to now, no systematic analysis on the connection between basic second-order and higher order compensation networks that can provide clear physical interpretations of the roles of extra components in higher order circuits has been reported.

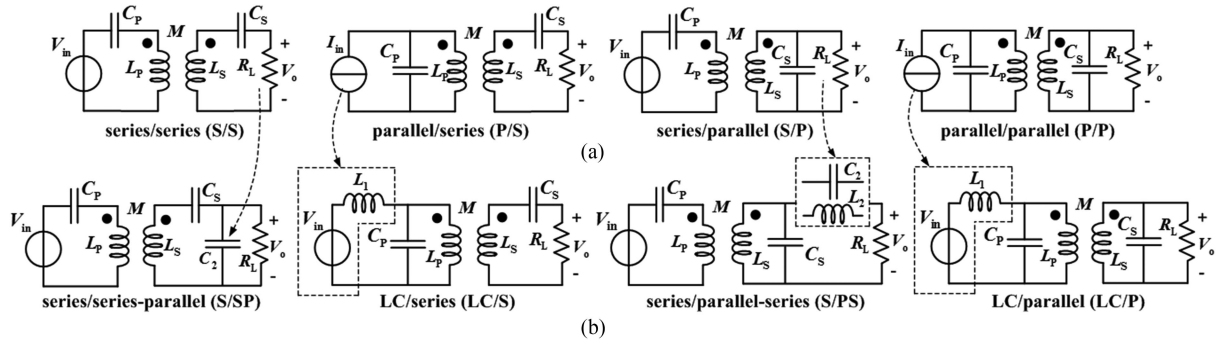


Fig. 1. Equivalent circuits of IPT converters with (a) basic second-order compensation circuits and (b) third-order compensation circuits with input voltage termination. Voltage and current sources are general independent sources, and are ac in the context of IPT converters.

In this article, we attempt to make a clear connection of higher order compensation circuits with the basic well-known second-order compensation circuits, thereby offering a convenient interpretation of the mechanism that contributes to the widened operating range. Specifically, we start with the common second-order compensation based on a two-port network model. Then, we explore the transformation of second-order compensation to third-order compensation through current source and voltage source interchange, together with LIC and LIV output conversion, which can be accomplished by adding an extra inductor or capacitor to the input or output of the original basic second-order compensation circuit. Furthermore, we examine the sensitivity of the basic second-order compensation circuits against input voltage and system parameters' variation in comparison to third-order compensation circuits. In this article, we focus our attention on practical applications where the input is fed by a voltage source. Thus, we consider the input voltage variation in the original basic second-order compensation circuit being translated to input *current* variation in the new third-order compensation circuit. Under this interpretation, we easily see that the extra inductor serves to convert the voltage source (which may be varying over a wide range) to a near constant current source. Thus, the widening in operating range can be systematically analyzed in terms of sensitivity of the circuits against input voltage variation.

In short, given the set of second-order compensation circuits being already so well understood, it is conceivable that general design pathways can be constructed by extension of the second-order compensation circuits, leading to specific third-order compensation circuits achieving specific improved features. Such design pathways should also provide a convenient circuit theoretic basis on which appropriate third or fourth-order compensation circuits can be conveniently constructed to meet the specific desired functions such as widening the input and load ranges and minimizing the effects of transformer misalignments.

This article is organized as follows. Section II provides a two-port model to illustrate basic transfer properties of IPT converters. Section III presents connection between basic second-order and third-order compensation circuits via extensions at input-side or output-side. Section IV provides a novel viewpoint based on sensitivity studies to infer useful design guidelines with clear physical meanings. Performances of various compensation

schemes in the event of input changes and transfer characteristics, with the required LIC or LIV output, are investigated and compared. In Section VI, experimental results are given for validation. Practical observations will be given throughout the article, offering useful interpretation of the roles of additional elements in higher order compensation. Finally, Section VII concludes the article.

II. COMPENSATION CIRCUITS

A. Basics

Shown in Fig. 1(a) are the four commonly known second-order compensation circuits for inductive power transfer. As dictated by Kirchhoff's laws, the input must be terminated by a voltage (current) source when series (parallel) compensation is applied at the primary side. Thus, from the circuit theoretic point of view, the S/S and S/P compensation circuits require an input voltage source, whereas the P/S and P/P compensation circuits require a current source feeding the input. Moreover, input voltage source is strictly prohibited for the P/S and P/P circuits unless an inductor is connected in series with it, as given in the LC/S and LC/P circuits shown in Fig. 1(b). These extended circuits are third-order compensation circuits and are rooted from the P/S and P/P circuits, though they can now be fed by an input voltage source, like the S/S and S/P circuits. Likewise, we can extend the S/S and S/P circuits at the load (secondary) side, resulting in third-order compensation circuits with voltage and current interchanged termination. As extra circuit parameters are available in the third-order compensation circuits, the possible operating ranges are expected to be widened, leading to improved design flexibility. In the following, we will evaluate these third-order circuits as extensions of the standard second-order compensation circuits in terms of their sensitivity to input voltage variation and parameter fluctuations. To keep our discussion practical, we will focus our attention on compensation circuits that are designed for input voltage termination.

B. Two-Port Network Model

To facilitate the analysis, the IPT converter is taken as a two-port network, as shown in Fig. 2. The converter is driven by a sinusoidal ac voltage source V_{in} , and loaded with an equivalent

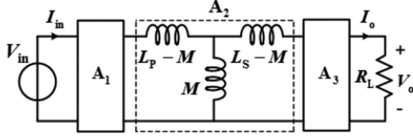


Fig. 2. Equivalent two-port network model of IPT converter with input voltage termination. A_1 is the primary-side compensation circuit, A_2 is the coupled inductor pair, and A_3 is the secondary-side compensation circuit. Voltage and current sources are general independent sources.

resistance R_L . Here, L_P and L_S denote self-inductance of the transformer at primary and secondary sides, respectively. Also, M is the mutual inductance between L_P and L_S , and ω is the operating frequency. The transfer characteristic of the network can be expressed as

$$\begin{bmatrix} V_{in} \\ I_{in} \end{bmatrix} = A \begin{bmatrix} V_o \\ I_o \end{bmatrix} \quad (1)$$

where A denotes the transmission matrix of the two-port network, and consists of three subnetworks, which are the primary compensation A_1 , the T-model equivalent transformer A_2 , and the secondary compensation A_3 . Thus, the second-order square matrix A can be obtained by

$$A = A_1 A_2 A_3 = \begin{bmatrix} a_{11} & j a_{12} \\ j a_{21} & a_{22} \end{bmatrix} \quad (2)$$

where a_{11} , a_{12} , a_{21} , and a_{22} are all real [20]. Using $I_o = V_o/R_L$, $Z_{in} = V_{in}/I_{in}$, and putting (2) in (1), the voltage gain G_v and transconductance G_i of the IPT circuit can be derived as

$$G_v = \frac{V_o}{V_{in}} = \frac{R_L}{a_{11} R_L + j a_{12}} \quad (3)$$

$$G_i = \frac{I_o}{V_{in}} = \frac{1}{a_{11} R_L + j a_{12}} \quad (4)$$

where R_L is the load resistance.

III. CONNECTING SECOND AND HIGHER ORDER COMPENSATION CIRCUITS

A. Input-Side Extension

Voltage sources are commonly utilized as the input sources at the primary side of IPT converters. With an additional inductor in series with the input voltage source, a near constant input current can be realized, which is equivalent to a current source, as shown in Fig. 3(a). Specifically, the equivalent current source reduces the order of compensation network from third-order to second-order. In this case, the input-side series inductor L_1 serves a unique role in maintaining a near constant or less fluctuated current, as well as in reducing the sensitivity to input variation. Thus, the design of the matching compensation circuits in primary and secondary sides can be based on the current source compensation.

Application of routine circuit analysis gives the input impedance of LC/S and LC/P compensation circuits shown in Fig. 1 as

$$Z_{in} = j\omega L_1 + \frac{1}{j\omega C_P} \parallel \left(j\omega L_P + \frac{\omega^2 M^2}{Z_S} \right) \quad (5)$$

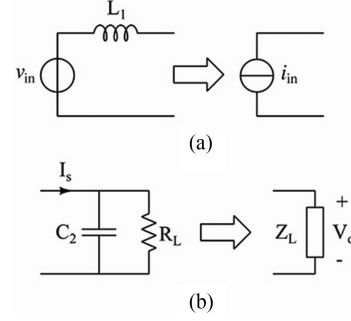


Fig. 3. Transformation of (a) input voltage source to input current source and (b) LIC output to LIV output between second-order and third-order compensations.

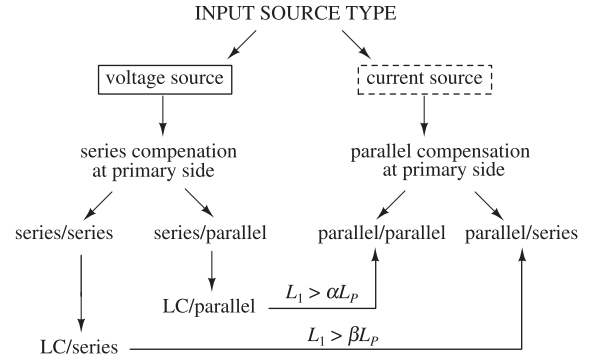


Fig. 4. Transformation from second-order to third-order compensation at primary side.

where $Z_{S-S} = j\omega L_S + \frac{1}{j\omega C_S} + R_L$ for the LC/S compensated circuit, and $Z_{S-P} = j\omega L_S + \frac{1}{j\omega C_S} \parallel R_L$ for the LC/P compensated circuit. Then, the input current of the LC/S compensated circuit can be calculated as

$$I_{in} = \frac{V_{in}}{j\omega (L_1 - L_P) + R_L L_P^2 / M^2}. \quad (6)$$

According to the properties listed in Table I, since the system operates at the resonance frequency, we can obtain the condition of L_1 of the LC/S compensated circuit for achieving near constant input current as follows:

$$k^2 (L_1 / L_P - 1) Q_{L-S} \gg 1. \quad (7)$$

Likewise, the L_1 in the LC/P compensated circuit should satisfy

$$\frac{k^2 L_1}{(1 - k^2)^2 L_P} Q_{L-P} \gg 1 \quad (8)$$

where Q_L denotes the quality factor of load. Also, $Q_{L-S} = \frac{\omega L_S}{R_L}$ and $Q_{L-P} = \frac{R_L}{\omega L_S}$.

Fig. 4 illustrates the basic compensation topologies according to the type of input source. The topologies for voltage source input include S/S and S/P compensation circuits, and those for current source input include P/P and P/S compensation circuits. Interchanging Thévenin and Norton representations, S/S circuits can be converted to P/S circuits when $L_1 > \beta L_P$, via LC/S circuit. Likewise, S/P circuits can be converted to P/P circuits when $L_1 > \alpha L_P$, via LC/P circuit. Here, α and β denote the

TABLE I
BASIC PROPERTIES OF VOLTAGE-INPUT COMPENSATION CIRCUITS UNDER LOAD-INDEPENDENT OUTPUT CONDITIONS (LIV OR LIC) AND HIGHER ORDER EXTENSIONS AT INPUT AND LOAD SIDES. $k = M/\sqrt{L_P L_S}$.

Type	Extension	Operating frequency	G_v at LIV or G_i at LIC	Input range	Tolerance of L_P variation	Tolerance of C_S variation	Coupling range (e.g., gap width, alignment)
S/S	basic	$\omega_o = \frac{1}{\sqrt{L_P C_P}} = \frac{1}{\sqrt{L_S C_S}}$	$G_i = \frac{1}{\omega_o M}$	narrow	–	high	narrow
S/S	basic	$\omega'_o = \frac{\omega_o}{\sqrt{1 \pm k}}$	$G_v = \sqrt{\frac{L_S}{L_P}}$	narrow	low	low	narrow
LC/S	L + P/S	$\omega_o = \frac{1}{\sqrt{L_P C_P}} = \frac{1}{\sqrt{L_S C_S}}$	$G_i \approx \frac{1}{j\omega_o M (\frac{L_1}{L_P} - 1)}$	extended	–	high	narrow
LC/S	L + P/S	$\omega'_o = \frac{1}{\sqrt{L_1 C_P}} = \frac{1}{\sqrt{L_S C_S}}$	$G_v \approx \frac{M}{L_1}$	extended	high	low	wide
SP/S	C + P/S	$\omega_o = \frac{1}{\sqrt{L_P (C_1 + C_P)}} = \frac{1}{\sqrt{L_S C_S}}$	$G_v = j \frac{\omega_o L_P C_1}{M}$	narrow	–	high	narrow
S/SP	S/S + C	$\omega_o = \frac{1}{\sqrt{L_P C_P}} = \frac{1}{\sqrt{L_S C_S}}$	$G_v \approx \frac{1}{\omega_o^2 M C_2}$	narrow	medium	high	wide
S/P	basic	$\omega_o = \frac{1}{\sqrt{L_P C_P (1 - k^2)}} = \frac{1}{\sqrt{L_S C_S}}$	$G_v = \frac{L_S}{M}$	narrow	–	high	narrow
S/P	basic	$\omega'_o = \frac{\omega_o}{\sqrt{1 \pm k}}$	$G_i = \frac{1}{\omega'_o L_S}$	narrow	low	low	narrow
LC/P	L + P/P	$\omega_o = \frac{1}{\sqrt{L_P C_P (1 - k^2)}} = \frac{1}{\sqrt{L_S C_S}}$	$G_v \approx \frac{(1 - k^2) M}{k^2 L_1}$	extended	–	low	narrow
LC/P	L + P/P	$\omega'_o = \frac{1}{\sqrt{L_1 C_P}} = \frac{1}{\sqrt{L_S C_S}}$	$G_i = \frac{M}{j\omega'_o L_1 L_S}$	extended	high	low	wide
SP/P	C + P/P	$\omega_o = \frac{1}{\sqrt{L_P (C_1 + C_P)}} = \frac{1}{\sqrt{L_S C_S}}$	$G_v = j \frac{\omega_o L_P C_1}{M}$	narrow	–	high	narrow
S/PS	S/P + C	$\omega_o = \frac{1}{\sqrt{L_P C_P (1 - k^2)}} = \frac{1}{\sqrt{L_S C_S}}$	$G_i \approx \frac{\omega_o L_S C_2}{jM}$	narrow	medium	high	wide
S/CL	S/P + L	$\omega_o = \frac{1}{\sqrt{L_P C_P (1 - k^2)}} = \frac{1}{\sqrt{L_S C_S}}$	$G_i \approx \frac{L_S}{j\omega_o M L_2}$	narrow	low	high	wide
LC/CL	L+P/P+L	$\omega_o = \frac{1}{\sqrt{L_P C_P}} = \frac{1}{\sqrt{L_S C_S}}$	$G_i \approx \frac{M}{j\omega_o L_S L_1}$	extended	high	medium	wide

ratio of L_1 to L_P . In practice, the constant input current can be achieved when α or β exceeds 10 [22]. The main function of L_1 is to realize a near constant current input, and hence to ensure that the compensation network works well over wider input and load variation ranges.

B. Load-Side Extension

The principle of voltage-current interchange can be applied at the load side in a likewise manner. For the LIC output scenario, with an additional capacitor in parallel with the load R_L , as shown in Fig. 3(b), the output voltage can be kept nearly constant. Similarly, in a third-order compensation network, with C_2 connected in parallel with R_L , the combined $C_2 \parallel R_L$ load serves as an equivalent capacitive load Z_L , which reduces the order of compensation circuit to second-order. In this case, the secondary-side parallel capacitor C_2 converts the LIC output to an LIV output by extending the second-order compensation to third-order compensation.

In order to achieve a constant output, basic operating conditions listed in Table I should be satisfied. For the S/SP circuit extended from an S/S circuit, using (2) and (3), the voltage gain can be expressed as

$$G_{v-S/SP} = \frac{1}{\omega^2 M C_2 \left(1 - \frac{j}{\omega C_2 R_L}\right)}. \quad (9)$$

It can be readily obtained that S/SP compensated circuit can achieve LIV output when

$$\omega C_2 R_L \gg 1. \quad (10)$$

Likewise, for S/PS circuit extended from S/P circuit, the transconductance can be calculated as

$$G_{i-S/PS} = \frac{L_S}{R_L M \left(1 + \frac{j\omega L_2}{R_L}\right)}. \quad (11)$$

To achieve LIC output, the system parameters need to satisfy

$$\frac{\omega L_2}{R_L} \gg 1. \quad (12)$$

Based on the above extension at both the input side and the output side, a fourth-order LC/CL compensation can be obtained, with operating conditions and transfer characteristics shown in Table I. The above theoretical analysis shows that when operating at a fixed frequency, a larger capacitor (inductor) in parallel (series) at the load side helps maintain a constant output voltage (current).

IV. SENSITIVITY ANALYSIS

In this section, we compare basic second-order compensation circuits with the extended compensation circuits in terms of the sensitivity against system parameters' fluctuation, the aim being

to establish the performance difference between higher order and second-order compensation circuits.

From (3) and (4), we see that the circuit can achieve LIV output when $a_{12} = 0$, and LIC output when $a_{11} = 0$. Thus, the transfer characteristics that satisfy load-independent (LI) output conditions can be obtained, as shown in Table I, where LC/S (LC/P) denotes compensation with inductor-capacitor on the primary side and a capacitor in series (parallel) on the secondary side, S/CL denotes compensation with a capacitor in series on the primary side and capacitor-inductor on the secondary side.

To compare the differences of extended higher order compensations with basic second-order compensations in terms of the influence to output when system parameters fluctuate, here we define the sensitivity of topology A's output against variation of parameter x as $S(x)_A$, i.e., for voltage output cases, we have

$$S_v(x)_A = \left| \frac{\Delta V_o(x)_A}{\Delta x} \right|. \quad (13)$$

Then, the sensitivity ratio of topology A to topology B with LIV output against variation of x can be expressed as

$$\lambda_v(x)_{A-B} = \frac{S_v(x)_A}{S_v(x)_B} = \left| \frac{\Delta V_o/\Delta x|_A}{\Delta V_o/\Delta x|_B} \right|. \quad (14)$$

A. Sensitivity to Input Voltage

According to (13) and (14), the sensitivity ratio λ of LC/P compensation circuits to S/P compensation circuits against input voltage variation can be expressed as

$$\lambda_v(V_{in})_{LCP-SP} = \frac{\left. \frac{\Delta V_o}{\Delta V_{in}} \right|_{LC/P}}{\left. \frac{\Delta V_o}{\Delta V_{in}} \right|_{S/P}} = \frac{G_{v-LC/P}}{G_{v-S/P}}. \quad (15)$$

Thus, for input voltage variation, the LC/P circuit is less sensitive than the S/P circuit when $\lambda_i(V_{in})_{LC/P-S/P} < 1$. Likewise, the LC/S circuit is less sensitive than the S/S circuit when $\lambda_v(V_{in})_{LC/S-S/S} < 1$. According to the expressions of transfer ratios listed in Table I, the above conditions can be further expressed as

$$\begin{aligned} L_1 > 2L_P &\Rightarrow \text{LC/S less sensitive than S/S for LIC} \\ L_1 > kL_P &\Rightarrow \text{LC/S less sensitive than S/S for LIV} \\ L_1 > M &\Rightarrow \text{LC/P less sensitive than S/P for LIC} \\ L_1 > (1 - k^2)L_P &\Rightarrow \text{LC/P less sensitive than S/P for LIV.} \end{aligned} \quad (16)$$

The connection between third-order compensation and second-order compensation can be conveniently established in terms of the sensitivity ratios. Here, we clearly see that compared with the second-order S/S circuit, the extended third-order LC/S and LC/P circuits have a widened input voltage range, by virtue of their input current source characteristic.

B. Sensitivity to Transformer and Compensation Parameters

Based on the above analytical results of LI output expressions and corresponding conditions, the impacts of variations of system parameters L_P , C_S , and k are considered in this section.

TABLE II
PARAMETERS OF IPT CIRCUITS FOR SIMULATION

Parameter	S/S	LC/S	S/SP	S/P	LC/P	S/PS	S/CL	LC/CL
L_P [μH]	76	76	76	76	76	76	76	76
L_S [μH]	76	76	76	76	76	76	76	76
L_1 [μH]	-	76	-	-	52.8	-	-	76
L_2 [μH]	-	-	-	-	-	-	76	76
C_P [nF]	33.3	33.3	33.3	47.9	47.9	47.9	47.9	33.3
C_S [nF]	33.3	33.3	33.3	33.3	33.3	33.3	33.3	33.3
C_2 [nF]	-	-	300	-	-	33.3	-	-
k	0.55	0.55	0.55	0.55	0.55	0.55	0.55	0.55
f [kHz]	100	100	100	100	100	100	100	100
V_{in-pp} [V]	50	50	50	50	50	50	50	50
r_p, r_s [Ω]	1	1	1	1	1	1	1	1
R_L [Ω]	10	10	10	10	10	10	10	10

Based on the definition given in (13) and (14), the sensitivity with respect to specific parameters for the topologies listed in Table I can be obtained. For parameters at the primary side, C_P is a designed parameter (value) determined by the operating condition as listed in Table I. We will assess the variation of L_P (transformer parameter) which is considered as system parameter here. Taking LC/S and S/S circuits with LIV output as examples, we substitute the G_v expressions of LC/S and S/S in Table I by (13) and (14), the sensitivity ratio with respect to L_P fluctuation is given by

$$\lambda_v(L_P)_{LC/S-S/S} = \frac{kL_P}{L_1} \quad (17)$$

According to the analysis given in Section III, the inductance of L_1 should be larger than L_P to achieve the desired constant input current. Thus, it can be readily observed that $\lambda_v(L_P)_{LC/S-S/S}$ is always less than one, meaning that an IPT converter compensated with LC/S performs better in tolerance and robustness than the S/S counterpart when L_P fluctuates. Similarly, S/P circuits with input-side extension, and other output-side extension can also be analyzed and compared in terms of the sensitivity to L_P , as shown in Table I. Fig. 5(a) and (b) illustrates the effects on the transfer ratio of various compensation networks when L_P changes, using the data listed in Table II. Normalization of data is applied here to clearly see the differences of sensitivity among the topologies. Both analytical and simulated results show that for the LIV output situation, the LC/S compensated circuit presents a higher tolerance to L_P variation compared to the S/S counterpart under the same operating condition. Likewise, for the LIC output situation, the LC/P and LC/CL compensated circuits perform better than the S/P circuit in terms of the tolerance to L_P variation under the same operating condition. This reveals that the input-side extension can be applied to widen the tolerance range of parameters and thus improve the robustness of the system during operation.

For parameters at the secondary side, assuming that the priority of achieving load-independent (LI) output is higher than that of zero phase angle input, the effects of capacitor C_S 's fluctuation are discussed as follows.

Take the S/S and the extended S/SP compensation circuits as examples. For the S/S compensated circuit with LIC output, according to the transfer matrix given in Section III and (3), LIC

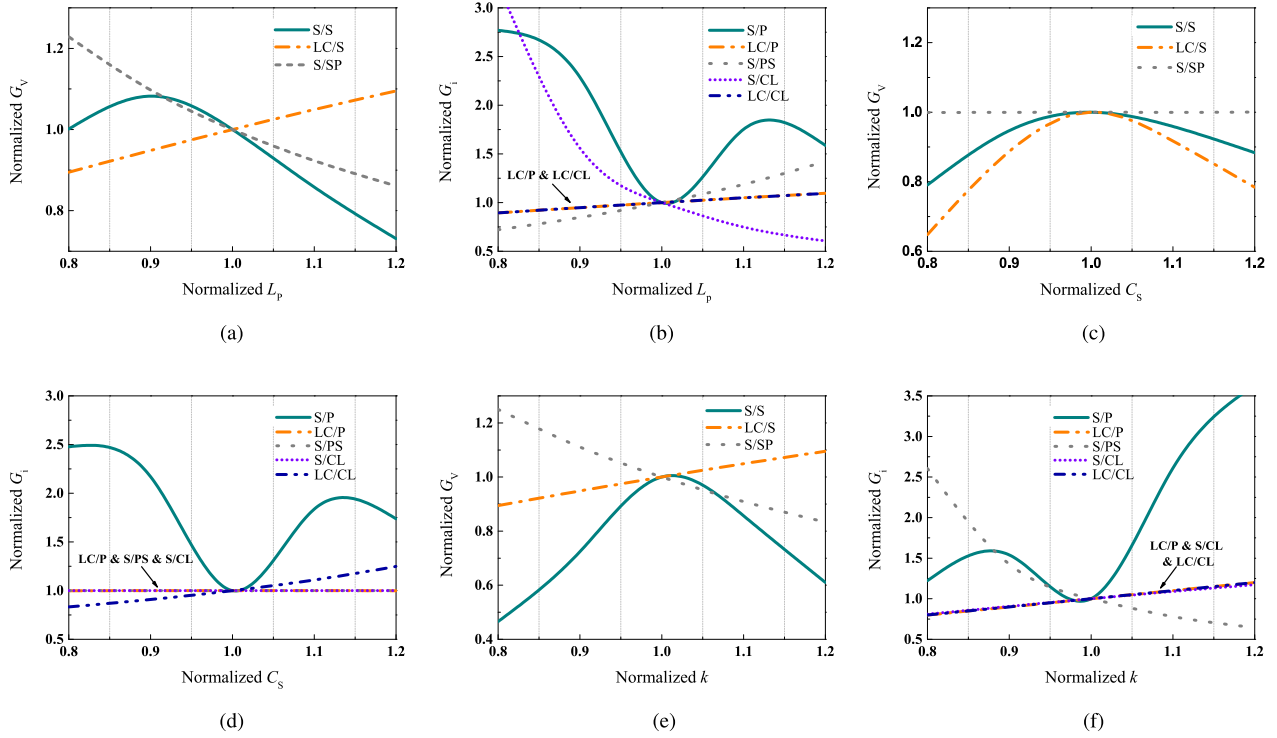


Fig. 5. (a) Normalized voltage gain versus normalized primary inductor L_P for S/S, LC/S, and S/SP compensated IPT circuits with LIV output. (b) Normalized transconductance versus normalized primary inductor L_P for S/P, LC/P, S/PS, S/CL, and LC/CL compensated IPT circuits with LIC output. (c) Normalized voltage gain versus normalized secondary capacitor C_S for S/S, LC/S, and S/SP compensated IPT circuits with LIV output. (d) Normalized transconductance versus normalized secondary capacitor C_S for S/P, LC/P, S/PS, S/CL, and LC/CL compensated IPT circuits with LIC output. (e) Normalized voltage gain versus normalized coupling coefficient k for S/S, LC/S, and S/SP compensated IPT circuits with LIV output. (f) Normalized transconductance versus normalized coupling coefficient k for S/P, LC/P, S/PS, S/CL, and LC/CL compensated IPT circuits with LIC output.

can be achieved by satisfying

$$a_{11} = \frac{L_P}{M} - \frac{1}{\omega^2 M C_P} = 0. \quad (18)$$

Now, putting (18) in (4), the transfer ratio G_i can be found as

$$G_{i-S/S} = j \frac{1}{\omega M} \quad (19)$$

which is also given in Table I. It can be readily observed from the above calculation that secondary compensated capacitor C_S has almost no effect on the S/S compensation with LIC output. However, in the LIV output scenario, substituting the primary compensation condition and the operating frequency into (3), we get the LIV condition as

$$a_{12} = \frac{j k L_P (\omega_o^2 L_S C_S - 1)}{\omega M C_S} \quad (20)$$

which means that the transfer ratio of S/S compensation with LIV output varies with the variation of C_S .

For the S/SP compensated circuit, since LIV output can be achieved with operating parameters of the basic S/S circuit with LIC output, the corresponding LIV condition is the same as given in (18). Combining with G_v expression in (9), it can be observed that the output of the S/SP compensated circuit is theoretically independent of the C_S value.

Likewise, the S/P compensated circuit with output-side extension and with other input-side extension can also be analyzed in

terms of the sensitivity to C_S , as shown in Table I. To illustrate the theoretical results more clearly, numerical simulations are performed, as given in Figs. 5(c) and 5(d). The parameters listed in Table II are used in the calculations. From Fig. 5(c), the results reveal that by adding a capacitor in parallel at the output side, the S/S compensated circuit can convert LIC to LIV output, still maintaining a high tolerance to C_S fluctuation. Similarly, Fig. 5(d) shows that with an additional capacitor or inductor in series at the output side, the conversion of LIV to LIC preserves the high tolerance to C_S variation of the S/P compensated circuit.

Based on the above analysis, it can be observed that various compensation networks possess different sensitivities to transformer parameter changes. In practice, apart from the fluctuation in circuit components, the gap width and lateral misalignment between the primary coil and the secondary coil may also vary during the operation. Such changes can be considered as variation in coupling coefficient k . According to Table I and (3), the S/SP compensated circuit can achieve higher voltage gain than the S/S compensated circuit when the system parameters satisfy

$$\omega^2 M C_2 < 1. \quad (21)$$

Considering that the operating frequency ω and capacitor C_2 need to meet the LIV condition, as per (10), requiring a relatively large value of C_2 when ω is fixed, the above condition can be

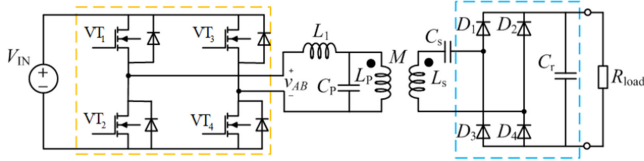


Fig. 6. Experimental LC/S compensated IPT converters.

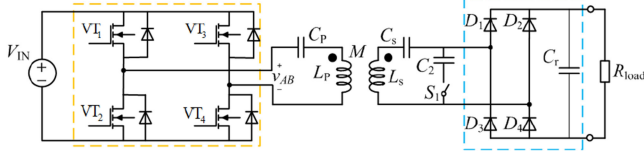


Fig. 7. Experimental S/S and extended S/SP compensated IPT converters.

TABLE III
PARAMETERS OF IPT CIRCUITS FOR EXPERIMENTS
UNDER LIV OUTPUT CONDITION

Parameters	S/S-LIV	S/S-LIC	LC/S	S/SP
L_P [μ H]	75.76	75.76	75.76	75.76
L_S [μ H]	76.85	76.85	76.85	76.85
C_P [nF]	33.43	33.43	33.43	33.43
C_S [nF]	32.96	32.96	32.96	32.96
L_1 [μ H]	NA	NA	76.20	NA
C_2 [nF]	NA	NA	NA	320.6
k	0.552	0.552	0.552	0.552
f [kHz]	149.4	100	100	100
V_{in-pp} [V]	50	50	50	50

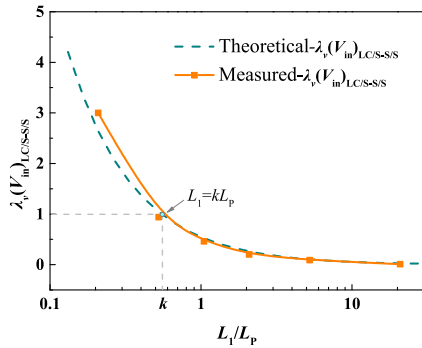


Fig. 8. Ratio of input-voltage-to-output-voltage sensitivity of LC/S to that of S/S compensation circuits.

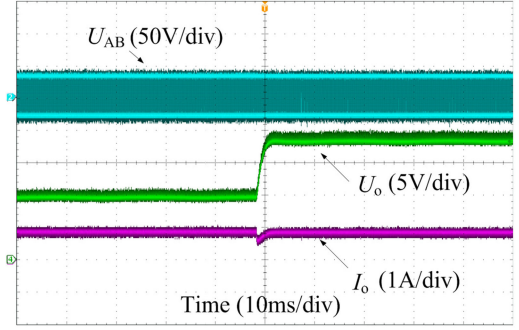
further expressed as

$$M < \frac{1}{\omega^2 C_2}. \quad (22)$$

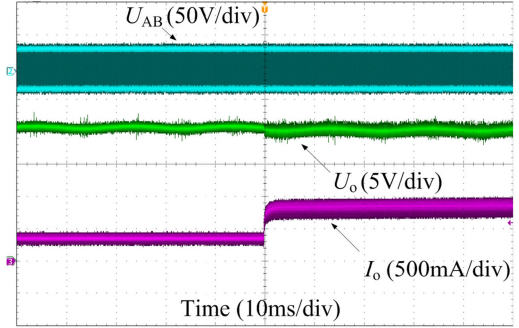
Likewise, for the S/PS compensated circuit, comparing the output expressions listed in Table I, a higher output current can be obtained if

$$\frac{L_S^2}{M L_2} > 1. \quad (23)$$

Analytical results are shown graphically in Fig. 5(e) and (f), which shows explicitly that the S/SP compensated circuit performs better in transferring higher voltage than the S/S compensated circuit with same system parameters and loosely coupled transformers. Moreover, the S/PS compensated circuit



(a)



(b)

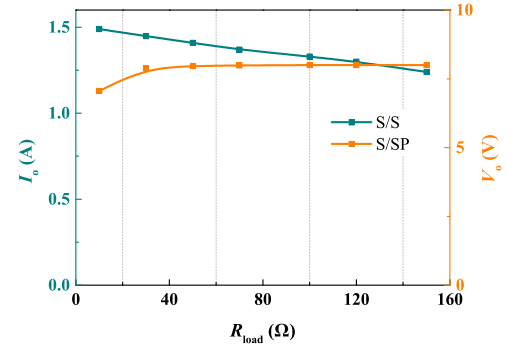
Fig. 9. Experimental waveforms of (a) S/S compensated and (b) S/SP compensated IPT converters when load resistance varies from 10 Ω to 50 Ω .

Fig. 10. Output current or voltage versus load resistance for S/S and S/SP compensated IPT converters showing sensitivity to load change.

possesses a higher transconductance than the S/P circuit under the same operating condition.

V. GENERAL PATHWAYS TO HIGHER ORDER COMPENSATION CIRCUITS

From the foregoing discussions, we can readily connect systematically the basic second-order compensation circuits and the higher order compensation circuits according to the extensions and the expected characteristics. First, we recognize that a higher order circuit allows more flexibility in design due to the extended parameter set, and if appropriate values of parameters and topologies are chosen, desirable characteristics can be achieved, as summarized below for the input voltage terminated IPT circuits.

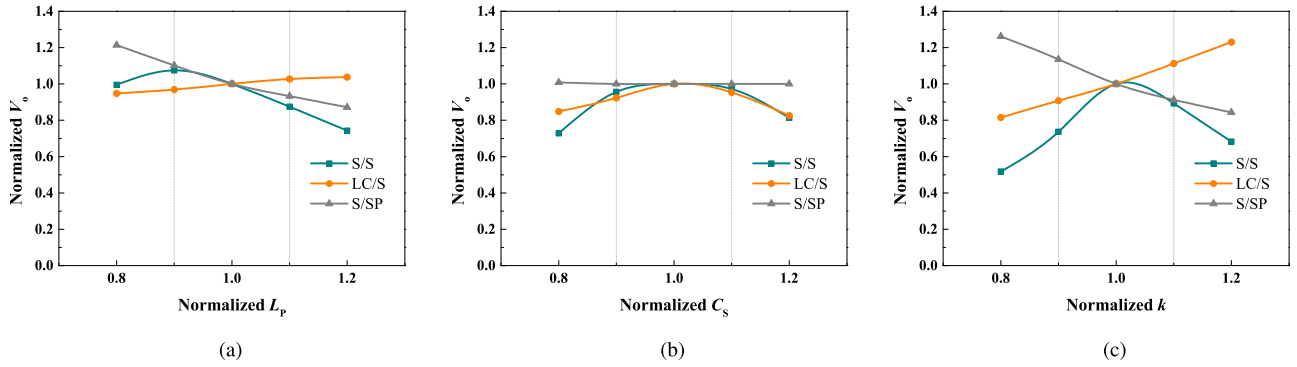


Fig. 11. Measured normalized voltage gain versus (a) normalized L_P , (b) normalized C_S , and (c) normalized coupling coefficient k of S/S, LC/S, and S/SP compensated IPT converters.

- 1) The S/S and S/P compensation circuits are the two basic types of compensation circuits that cater for input voltage termination.
- 2) Sensitivity to variation in the input voltage and primary inductance improves significantly if the input is converted to a current source by connecting upfront an inductor in series. The resulting circuits are LC/S and LC/P configurations, which are effectively current-fed P/S and P/P circuits. The range of input voltage is widened due to the near constant input current. The extended circuits become more tolerant to inductance L_P fluctuation because of the change of compensation conditions at the primary side.
- 3) The output-side LIC-LIV and LIV-LIC conversions contribute to maintaining the high tolerance to fluctuation of the compensation component C_S . Specifically, the S/S topology achieves LIC with optimized low sensitivity to C_S fluctuation. To preserve the simple advantage but serve an LIV application, one may extend the secondary side to S/SP to achieve LIV, which preserves the near zero sensitivity to C_S variation.
- 4) The input-side and output-side extensions based on the basic second-order compensation topologies can be systematically applied to widen the coupling range, and hence to provide a higher degree of freedom for choosing parameter values. Specifically, output-side extensions perform well with loosely coupled transformers. This means that in situations where high capacity is needed to address varying misalignment and transfer gap, the output-side extension topologies can be considered.

VI. EXPERIMENTAL VALIDATION

To validate the analysis presented above, S/S, LC/S, and S/SP compensation circuits are constructed, as shown in Figs. 6 and 7. The inverter, shown in the yellow dashed box, consists of MOSFET VT_1 to VT_4 , using C2M0080120. The rectifier, shown in the blue dashed box, consists of diodes D_1 to D_4 which are implemented by IDH08G65C6XKSA. The filter capacitor C_r is 5 μ F. The specific parameters listed in Table III are used in our experiments.

Fig. 8 shows the analytical and measured sensitivity ratio of LC/S circuit to S/S circuit against input voltage variation under

LIV output condition. Compared with the analytical results of $\lambda_v(V_{in})_{LC/S-S/S}$, the measured results show a higher sensitivity when L_1 is small. The reason is that a small series inductor does not guarantee near constant input current, and the sensitivity of the circuit with an input-side inductor will change dramatically when the inductance value is small. When the value of $\lambda_v(V_{in})_{LC/S-S/S}$ equals 1, the sensitivity of the output to input voltage variation of the LC/S topology is the same as that of the S/S topology.

Fig. 9(a) and (b) shows the transient waveforms when the load resistance is stepped from 10 Ω to 50 Ω in the S/S compensated converter, and the S/SP compensated converter is extended by S/S compensation, respectively. It is found that the output current of the S/S converter and the output voltage of the S/SP converter are almost unchanged as the load resistance varies. This matches well with the analytical results. Fig. 10 shows the measured output current of the S/S compensated converter and the output voltage of the S/SP compensated converter versus the load resistance. The results show that by adding a capacitor in parallel at the output side, a constant current output can be converted to a constant voltage output.

To facilitate comparison of different topologies, normalized values are used. In particular, we normalize values of inductance, capacitance, and coupling coefficient with respect to the resonant point, with the corresponding voltage gain and transconductance being set to 1. Thus, the universal range from 0.8 to 1.2 can be used for comparison instead of the actual values. Fig. 11(a)–(c) demonstrates the measured normalized voltage gain versus the normalized value of L_P , C_S , and k of the experimental S/S, LC/S, and S/SP compensated converters with LIV output, respectively. Here, the variation of the value of k is achieved by changing the gap of the transformer in the IPT converter. It can be readily observed from Fig. 11(a) that the LC/S topology is capable of maintaining a relatively constant output for a larger L_P variation. This means that the input-side extension helps to make the IPT converter less sensitive against variation of L_P at the primary side. Likewise, in Fig. 11(b), when the normalized value of C_S changes from 0.8 to 1.2, the normalized voltage gain of the S/SP compensated converter changes very little compared with the other two converters, verifying that the output-side extension serves to reduce the system sensitivity to variation of C_S at the secondary side. Fig. 11(c) illustrates that when k

decreases, the voltage gain of the S/SP topology increases, while the other two topologies show different rates of decline in voltage gain. Thus, compared with second-order compensated circuits and their input-side extensions, the output-side extensions perform better in maintaining constant output voltage when the transformer has a loose coupling or large misalignment. The above experimental results agree with the analytical results.

Thus, we have clearly seen the connection from second-order to third-order compensation circuits, and the parameter conditions under which both widening the range of input voltage and converting LIC output to LIV output can be achieved. In addition, the system sensitivity of output to parameter fluctuations are shown to be improved by extending second-order to higher order compensations.

VII. CONCLUSION

The literature abounds with numerous design examples of higher order compensation circuits for inductive power transfer converters that address the variation of parameters and improve the operating range for the applications concerned. It is generally accepted that higher order circuits offer better flexibility and higher degree of design freedom by expanding the parameter space. Specific applications require combating variation of specific variables or parameters such as input voltage variation, load variation, and transformer's coupling variation. In much of the reported work, specific topologies were proposed with detailed analytical equations derived corresponding to the specific topologies. However, a general circuit theoretic pathway leading to a suitable design for specific application is neither available nor well understood.

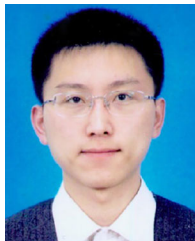
This article presents a new perspective of higher order compensation circuits based on sensitivity analysis, and compares the sensitivities of various compensation topologies with the basic second-order compensation circuits in terms of input voltage change, design parameter change, and coupling range. The analysis presented here provides a convenient connecting pathway from second-order circuits to higher order circuits, mapping each type of topological extension with the specific performance outcome. In practice, the presented analysis offers a quick design guideline for deriving higher order compensation circuits capable of enhancing specific performance areas such as widening of input and load ranges. Specifically, the results show that adding an inductor or capacitor at input side and output side of a second-order circuit in specific fashions can effectively reduce the sensitivity of the system to parameter variation, provided the added inductor or capacitor exceeds a certain value. In addition, with higher order compensation at the output side, the system can achieve a higher voltage gain. Furthermore, with a certain range of the inductance in series (or capacitance in parallel), a voltage source (constant current output) can be made equivalent to a constant current source (constant voltage output). The proposed perspective of topological extension from second-order compensated circuits offers a simple and effective basis for understanding how higher order compensation circuits combat parameter variation.

REFERENCES

- [1] G. A. Covic and J. T. Boys, "Inductive power transfer," *Proc. IEEE*, vol. 101, no. 6, pp. 1276–1289, Aug. 2013.
- [2] M. Budhia, J. T. Boys, G. A. Covic, and C. Huang, "Development of a single-sided flux magnetic coupler for electric vehicle IPT charging systems," *IEEE Trans. Ind. Electron.*, vol. 60, no. 1, pp. 318–328, Jan. 2013.
- [3] A. Zaheer, G. A. Covic, and D. Kacprzak, "A bipolar pad in a 10-kHz 300 W distributed IPT system for AGV applications," *IEEE Trans. Ind. Electron.*, vol. 61, no. 7, pp. 3288–3301, Jul. 2014.
- [4] S. Li, W. Li, and C. Mi, "A double-sided LCC compensation network and its tuning method for wireless power transfer," *IEEE Trans. Power Electron.*, vol. 64, no. 6, pp. 2261–2273, Jun. 2015.
- [5] C. T. Rim and C. Mi, *Wireless Power Transfer for Electric Vehicles and Mobile Devices*. New York, NY, USA: Wiley-IEEE Press, 2018.
- [6] A. Hussein and I. Batarseh, "A review of charging algorithms for nickel and lithium battery chargers," *IEEE Trans. Veh. Technol.*, vol. 60, no. 3, pp. 830–838, Mar. 2011.
- [7] F. Musavi and W. Eberle, "Overview of wireless power transfer technologies for electric vehicle battery charging," *IET Power Electron.*, vol. 7, no. 7, pp. 60–66, Jan. 2014.
- [8] W. Zhang, S. C. Wong, C. K. Tse, and Q. Chen, "Load-independent duality of current and voltage outputs of a series or parallel compensated inductive power transfer converter with optimized efficiency," *IEEE J. Emerg. Select. Topics Power Electron.*, vol. 3, no. 1, pp. 137–146, Jan. 2015.
- [9] X. Qu, H. Han, S. C. Wong, and C. K. Tse, "Hybrid IPT topologies with constant-current or constant-voltage output for battery charging applications," *IEEE Trans. Power Electron.*, vol. 30, no. 11, pp. 6129–6337, Nov. 2015.
- [10] W. Zhang and C. Mi, "Compensation topologies of high-power wireless power transfer systems," *IEEE Trans. Veh. Technol.*, vol. 65, no. 6, pp. 4768–4778, Jun. 2016.
- [11] S. Wang, J. Chen, Z. Hu, C. Rong, and M. Liu, "Optimisation design for series-series dynamic WPT system maintaining stable transfer power," *IET Power Electron.*, vol. 10, no. 9, pp. 987–995, Jul. 2017.
- [12] Q. Zhu, L. Wang, C. Liao, and F. Li, "Improving the misalignment tolerance of wireless charging system by optimizing the compensate-capacitor," *IEEE Trans. Ind. Electron.*, vol. 62, no. 8, pp. 4832–4836, Aug. 2015.
- [13] J. Hou, Q. Chen, S. C. Wong, C. K. Tse, and X. Ruan, "Analysis and control of series/series-parallel compensated resonant converters for contactless power transfer," *IEEE J. Emerg. Select. Topics Power Electron.*, vol. 3, no. 1, pp. 124–136, Mar. 2015.
- [14] X. Qu, Y. Jing, H. Han, S. C. Wong, and C. K. Tse, "Higher order compensation for inductive-power-transfer converters with constant voltage or constant-current output combating transformer parameter constraints," *IEEE Trans. Power Electron.*, vol. 32, no. 1, pp. 394–405, Jan. 2017.
- [15] M. L. G. Kissin, C. Y. Huang, G. A. Covic, and J. T. Boys, "Detection of the tuned point of a fixed-frequency LCL resonant power supply," *IEEE Trans. Power Electron.*, vol. 24, no. 4, pp. 1140–1143, Apr. 2009.
- [16] U. K. Madawala and D. J. Thrimawithana, "Current sourced bi-directional inductive power transfer system," *IET Power Electron.*, vol. 4, no. 4, pp. 471–480, Apr. 2011.
- [17] J. T. Boys and G. A. Covic, "The inductive power transfer story at the University of Auckland," *IEEE Circuits Syst. Mag.*, vol. 15, no. 2, pp. 6–27, Jun. 2015.
- [18] A. Ramezani, S. Farhangi, H. Iman-Eini, B. Farhangi, R. Rahimi, and G. R. Moradi, "Optimized LCC-series compensated resonant network for stationary wireless EV chargers," *IEEE Trans. Ind. Electron.*, vol. 66, no. 4, pp. 2756–2765, Apr. 2019.
- [19] B. Esteban, M. Sid-Ahmed, and N. C. Kar, "A comparative study of power supply architectures in wireless EV charging systems," *IEEE Trans. Power Electron.*, vol. 30, no. 11, pp. 6408–6417, Nov. 2015.
- [20] X. Qu, H. Chu, S. C. Wong, and C. K. Tse, "An IPT battery charger with near unity power factor and load-independent constant output combating design constraints of input voltage and transformer parameters," *IEEE Trans. Power Electron.*, vol. 34, no. 8, pp. 7719–7727, Aug. 2019.
- [21] J. Lu, G. Zhu, H. Wang, F. Lu, J. Jiang, and C. Mi, "Sensitivity analysis of inductive power transfer systems with voltage-fed compensation topologies," *IEEE Trans. Veh. Technol.*, vol. 68, no. 5, pp. 4502–4513, May 2019.
- [22] Y. Liu, C. K. Tse, C. Zhu, and S. C. Wong, "Comparison of second-order and third-order compensation of inductive power transfer converters based on sensitivity analysis," in *Proc. IEEE Int. Symp. Circuits Syst.*, Oct. 2020, pp. 1–5.



Ying Cathy Liu (Student Member, IEEE) received the B.Eng. and M.Sc. degrees in electrical engineering from the Harbin Institute of Technology, Harbin, China, in 2014 and 2016, respectively. She is currently working toward the Joint Ph.D. Program with the Hong Kong Polytechnic University, Hong Kong, and the Harbin Institute of Technology, in the area of power electronics and wireless power transfer.



applied for aerospace, underwater, and flexible medical devices.

Jiantao Zhang (Fellow, IEEE) received the B.Eng., M.Sc., and Ph.D. degrees in electrical engineering from the Harbin Institute of Technology, Harbin, China, in 2009, 2011, and 2019, respectively. From 2014 to 2016, he was a Joint Ph.D. Student with École Polytechnique Fédérale de Lausanne, Lausanne, Switzerland, working on wireless power transfer for medical devices. He is now a Lecturer with the Department of Electrical Engineering and Automation, Harbin Institute of Technology. His current research interests include wireless power transfer



Chi K. Tse (Fellow, IEEE) received the B.Eng. degree (with first class honors) and the Ph.D. degree, both in electrical engineering, from the University of Melbourne, Melbourne, Australia, in 1987 and 1991, respectively.

He is presently the Chair Professor of Electrical Engineering with City University of Hong Kong, Hong Kong, and was the Chair Professor and Head of Electronic and Information Engineering with Hong Kong Polytechnic University, Hong Kong. His research interests include power electronics, nonlinear

systems, and complex network applications.

Dr. Tse serves and has served as the Editor-in-Chief for the IEEE TRANSACTIONS ON CIRCUITS AND SYSTEMS II (2016–2019), *IEEE Circuits and Systems Magazine* (2012–2015), and *IEEE Circuits and Systems Society Newsletter* (since 2007), Associate Editor for three IEEE Journal/Transactions, Editor for *International Journal of Circuit Theory and Applications*, and is on the editorial board of the IEEE PROCEEDINGS. He was the recipient of a number of research and industry awards, including Prize Paper Awards by IEEE TRANSACTIONS ON POWER ELECTRONICS in 2001, 2015, and 2017, RISP Journal of Signal Processing Best Paper Award in 2014, Best Paper Award by International Journal of Circuit Theory and Applications in 2003, two Gold Medals at the International Inventions Exhibition in Geneva in 2009 and 2013, a Grand Prize and Gold Medal at the Silicon Valley International Invention Festival in 2019, and a number of recognitions by the academic and research communities, including honorary professorship by several Chinese and Australian universities, Chang Jiang Scholar Chair Professorship, IEEE Distinguished Lectureship, Distinguished Research Fellowship by the University of Calgary, Gladden Fellowship, and International Distinguished Professorship-at-Large by the University of Western Australia.



Chunbo Zhu received the B.Eng. and M.Sc. degrees in electrical engineering, and the Ph.D. degree in mechanical engineering from the Harbin Institute of Technology (HIT), Harbin, China, in 1987, 1992, and 2001, respectively.

From 2003 to 2004, he was a Postdoctoral Research Fellow with the PEI Research Center, National University of Ireland, Galway, Ireland. Since 1987, he has been a Lecturer with the Department of Automation Measurement and Control, HIT. He is currently a Full Professor with HIT, where he leads the Laboratory of

Wireless Power Transfer and Battery Management Technologies. His current research interests include energy management systems, electric and hybrid electric vehicles, and wireless power transfer technologies.



Siu-Chung Wong (Senior Member, IEEE) received the B.Sc. degree in physics from the University of Hong Kong, Hong Kong, in 1986, the M.Phil. degree in electronics from the Chinese University of Hong Kong, Hong Kong, in 1989, and the Ph.D. degree from the University of Southampton, Southampton, U.K., in 1997.

In 1988, he joined The Hong Kong Polytechnic University, Hong Kong, as an Assistant Lecturer. He is currently an Associate Professor with the Department of Electronic and Information Engineering,

The Hong Kong Polytechnic University, where he conducts research in power electronics. From 2012 to 2015, he was a Chutian Scholar Chair Professor with the Hubei Provincial Department of Education, China, and the appointment was hosted by the Wuhan University of Science and Technology, Wuhan, China. In 2013, he was a Guest Professor with the School of Electrical Engineering, Southeast University, Nanjing, China. He was a Visiting Scholar with the Center for Power Electronics Systems, Virginia Tech, VA, USA, in November 2008, Aero-Power Sci-tech Center, Nanjing University of Aeronautics and Astronautics, Nanjing, China, in January 2009, and with the School of Electrical Engineering, Southeast University, in March 2012.

Dr. Wong is a member of the Electrical College, Institution of Engineers, Australia. He is an Editor for the *Energy and Power Engineering Journal* and a member of the Editorial Board of the *Journal of Electrical and Control Engineering*. He is a Guest Associate Editor for the *IEEE Journal of Emerging and Selected Topics in Power Electronics*, Special Issue on “Power Electronics for Biomedical Applications” in 2014 and an Associate Editor for the IEEE TRANSACTIONS ON CIRCUITS AND SYSTEMS II.